Measurement of $ep \to e^{'}p\pi^{+}\pi^{-}$ and baryon resonance analysis

M. Ripani,[1] V.D. Burkert,[2] V. Mokeev,[3] M. Battaglieri,[1] R. De Vita,[1] E. Golovach,[3] M. Taiuti,[1] G. Adams,[30] E. Anciant,[8] M. Anghinolfi,[1] B. Asavapibhop,[23] G. Audit,[8] T. Auger,[8] H. Avakian,[2,17] H. Bagdasaryan,[38] J.P. Ball,[4] S. Barrow,[14] K. Beard,[20] M. Bektasoglu,[27] B.L. Berman,[15] N. Bianchi,[17] A.S. Biselli,[30] S. Boiarinov,[2,19] B.E. Bonner,[31] S. Bouchigny,[18,2] R. Bradford,[6] D. Branford,[12] W.J. Briscoe,[15] W.K. Brooks,[2] J.R. Calarco,[24] D.S. Carman,[26] B. Carnahan,[7] A. Cazes,[33] C. Cetina,[15] L. Ciciani,[27] P.L. Cole,[34,2] A. Coleman,[37] D. Cords,[2] P. Corvisiero,[1] D. Crabb,[36] H. Crannell,[7] J.P. Cummings,[30] E. De Sanctis,[17] P.V. Degtyarenko,[2] H. Denizli,[28] L. Dennis,[14] K.V. Dharmawardane,[27] C. Djalali,[33] G.E. Dodge,[27] D. Doughty,[9,2] P. Dragovitsch,[14] M. Dugger,[4] S. Dytman,[28] M. Eckhause,[37] H. Egiyan,[37] K.S. Egiyan,[38] L. Elouadrhiri,[2] A. Empl,[30] R. Fatemi,[36] G. Fedotov,[3] G. Feldman,[15] R.J. Feuerbach,[6] J. Ficenec,[35] T.A. Forest,[27] H. Funsten,[37] S.J. Gaff,[11] M. Gai,[10] M. Garçon,[8] G. Gavalian,[24,38] S. Gilad,[22] G.P. Gilfoyle,[32] K.L. Giovanetti,[20] P. Girard,[33] K. Griffioen,[37] M. Guidal,[18] M. Guillo,[33] L. Guo,[2] V. Gyurjyan,[2] C. Hadjidakis,[18] J. Hardie,[9,2] D. Heddle,[9,2] P. Heimberg,[15] F.W. Hersman,[24] K. Hicks,[26] R.S. Hicks,[23] M. Holtrop,[24] J. Hu,[30] C.E. Hyde-Wright,[27] B. Ishkhanov,[3] M.M. Ito,[2] D. Jenkins,[35] K. Joo,[2,36] J.H. Kelley,[11] J.D. Kellie,[16] M. Khandaker,[25] K.Y. Kim,[28] K. Kim,[21] W. Kim,[21] A. Klein,[27] F.J. Klein,[7,2] A.V. Klimenko,[27] M. Klusman,[30] M. Kossov,[19] L.H. Kramer,[13,2] Y. Kuang,[37] S.E. Kuhn,[27] J. Kuhn,[30] J. Lachniet,[6] J.M. Laget,[8] D. Lawrence,[23] Ji Li,[30] K. Livingston,[16] A. Longhi,[7] K. Lukashin,[2] J.J. Manak,[2] C. Marchand,[8] S. McAleer,[14] J. McCarthy,[36] J.W.C. McNabb,[6] B.A. Mecking,[2] M.D. Mestayer,[2] C.A. Meyer,[6] K. Mikhailov,[19] R. Minehart,[36] M. Mirazita,[17] R. Miskimen,[23] L. Morand,[8] S.A. Morrow,[18] M.U. Mozer,[26] V. Muccifora,[17] J. Mueller,[28] L.Y. Murphy,[15] G.S. Mutchler,[31] J. Napolitano,[30] R. Nasseripour,[13] S.O. Nelson,[11] S. Niccolai,[15] G. Niculescu,[26] I. Niculescu,[15] B.B. Niczyporuk,[2] R.A. Niyazov,[27] M. Nozar,[2,25] G.V. O'Rielly,[15] A.K. Opper,[26] M. Osipenko,[3] K. Park,[21] E. Pasyuk,[4] G. Peterson,[23] S.A. Philips,[15] N. Pivnyuk,[19] D. Pocanic,[36] O. Pogorelko,[19] E. Polli,[17] S. Pozdniakov,[19] B.M. Preedom,[33] J.W. Price,[5] Y. Prok,[36] D. Protopopescu,[24] L.M. Qin,[27] B. Quinn,[6] B.A. Raue,[13,2] G. Riccardi,[14] G. Ricco,[1] B.G. Ritchie,[4] F. Ronchetti,[17,29] P. Rossi,[17] D. Rowntree,[22] P.D. Rubin,[32] F. Sabatié,[8,27] K. Sabourov,[11] C. Salgado,[25] J.P. Santoro,[35,2] V. Sapunenko,[1] R.A. Schumacher,[6] V.S. Serov,[19] A. Shafi,[15] Y.G. Sharabian,[2,38] J. Shaw,[23] S. Simionatto,[15] A.V. Skabelin,[22] E.S. Smith,[2] L.C. Smith,[36] D.I. Sober,[7] M. Spraker,[11] A. Stavinsky,[19] S. Stepanyan,[27,38] P. Stoler,[30] I.I. Strakovsky,[15] S. Taylor,[31] D.J. Tedeschi,[33] U. Thoma,[2] R. Thompson,[28] L. Todor,[6] M. Ungaro,[30] M.F. Vineyard,[32] A.V. Vlassov,[19] K. Wang,[36] L.B. Weinstein,[27] H. Weller,[11] D.P. Weygand,[2] C.S. Whisnant,[33] E. Wolin,[2] M.H. Wood,[33] A. Yegneswaran,[2] J. Yun,[27] B. Zhang,[22] J. Zhao,[22] Z. Zhou,[22]

[1] *INFN, Sezione di Genova, 16146 Genova, Italy*
[2] *Thomas Jefferson National Accelerator Facility, Newport News, Virginia 23606*
[3] *Moscow State University, 119899 Moscow, Russia*
[4] *Arizona State University, Tempe, Arizona 85287*
[5] *University of California at Los Angeles, Los Angeles, California 90095*
[6] *Carnegie Mellon University, Pittsburgh, Pennsylvania 15213*
[7] *Catholic University of America, Washington, D.C. 20064*
[8] *CEA-Saclay, Service de Physique Nucléaire, F91191 Gif-sur-Yvette, Cedex, France*
[9] *Christopher Newport University, Newport News, Virginia 23606*
[10] *University of Connecticut, Storrs, Connecticut 06269*
[11] *Duke University, Durham, North Carolina 27708*
[12] *Edinburgh University, Edinburgh EH9 3JZ, United Kingdom*
[13] *Florida International University, Miami, Florida 33199*
[14] *Florida State University, Tallahasee, Florida 32306*
[15] *The George Washington University, Washington, DC 20052*
[16] *University of Glasgow, Glasgow G12 8QQ, United Kingdom*
[17] *INFN, Laboratori Nazionali di Frascati, PO 13, 00044 Frascati, Italy*
[18] *Institut de Physique Nucleaire ORSAY, IN2P3 BP 1, 91406 Orsay, France*
[19] *Institute of Theoretical and Experimental Physics, Moscow, 117259, Russia*
[20] *James Madison University, Harrisonburg, Virginia 22807*
[21] *Kyungpook National University, Daegu 702-701, South Korea*
[22] *Massachusetts Institute of Technology, Cambridge, Massachusetts 02139*
[23] *University of Massachusetts, Amherst, Massachusetts 01003*
[24] *University of New Hampshire, Durham, New Hampshire 03824*
[25] *Norfolk State University, Norfolk, Virginia 23504*
[26] *Ohio University, Athens, Ohio 45701*
[27] *Old Dominion University, Norfolk, Virginia 23529*

[28] University of Pittsburgh, Pittsburgh, Pennsylvania 15260
[29] Universita' di ROMA III, 00146 Roma, Italy
[30] Rensselaer Polytechnic Institute, Troy, New York 12180
[31] Rice University, Houston, Texas 77005
[32] University of Richmond, Richmond, Virginia 23173
[33] University of South Carolina, Columbia, South Carolina 29208
[34] University of Texas at El Paso, El Paso, Texas 79968
[35] Virginia Polytechnic Institute and State University, Blacksburg, Virginia 24061
[36] University of Virginia, Charlottesville, Virginia 22901
[37] College of William and Mary, Williamsburg, Virginia 23187 and
[38] Yerevan Physics Institute, 375036 Yerevan, Armenia

(Dated: April 24, 2003)

The cross section for the reaction $ep \rightarrow e'p\pi^+\pi^-$ was measured in the resonance region for 1.4<W<2.1 GeV and 0.5< Q^2 <1.5 GeV^2/c^2 using the CLAS detector at Jefferson Laboratory. The data show resonant structures not visible in previous experiments. The comparison of our data to a phenomenological prediction using available information on N^* and Δ states shows an evident discrepancy. A better description of the data is obtained either by a sizeable change of the properties of the $P_{13}(1720)$ resonance or by introducing a new baryon state, not reported in published analyses.

PACS numbers: 13.60.Le, 13.40.Gp, 14.20.Gk

Electromagnetic excitation of nucleon resonances is sensitive to the spin and spatial structure of the transition, which in turn is connected to fundamental properties of baryon structure, like spin-flavor symmetries, confinement, and effective degrees of freedom. In the mass region above 1.6 GeV, many overlapping baryon states are present, and some of them are not well known; measurement of the transition form factors of these states is important for our understanding of the internal dynamics of baryons. Many of these high-mass excited states tend to decouple from the single-meson channels and to decay predominantly into multi-pion channels, such as $\Delta\pi$ or $N\rho$, leading to $N\pi\pi$ final states [1]. Moreover, quark models with approximate (or "broken") SU(6)$\otimes$O(3) symmetry [2, 3] predict more states than have been found experimentally; QCD mixing effects could decouple these unobserved states from the pion-nucleon channel [2] while strongly coupling them to two-pion channels [2, 4, 5]. These states would therefore not be observable in reactions with πN in the initial or final state. Other models, with different symmetry properties and a reduced number of degrees of freedom, as e.g. in ref. [6], predict fewer states. Experimental searches for at least some of the "missing" states predicted by the symmetric quark models, which are not predicted by models using alternative symmetries, are crucial in discriminating between these models. Electromagnetic amplitudes for some missing states are predicted to be sizeable [2] as well. Therefore, exclusive double-pion electroproduction is a fundamental tool in measuring poorly known states and possibly observing new ones.

In this paper we report a measurement of the $ep \rightarrow e'p\pi^+\pi^-$ reaction studied with the CEBAF Large Acceptance Spectrometer (CLAS) at Jefferson Lab. More details on the experimental and physical analysis can be found in [8]. Beam currents of a few nA were delivered to Hall B on a liquid-hydrogen target, corresponding to luminosities up to 4×10^{33} cm^{-2}s^{-1}. Data were taken in 1999 for about two months at beam energies of 2.6 and 4.2 GeV. Important features of the CLAS [7] are its large kinematic coverage for multi-charged-particle final states and its good momentum resolution ($\Delta p/p \sim$1%). Using an inclusive electron trigger based on a coincidence between the forward electromagnetic shower calorimeter and the gas Cerenkov detector, many exclusive hadronic final states were measured simultaneously. Scattered electrons were identified through cuts on the calorimeter energy loss and the Cerenkov photo-electron distribution. Different channels were separated through particle identification using time-of-flight information and other kinematic cuts. We used the missing-mass technique, requiring detection in CLAS of at least $ep\pi^+$. The good resolution allowed selection of the exclusive final state, $ep\pi^+\pi^-$. After applying all cuts, our data sample included about 2×10^5 two-pion events.

The range of invariant hadronic center-of-mass (CM) energy W (in 25 MeV bins) was 1.4-1.9 GeV for the first two bins in the invariant momentum transfer Q^2, 0.5-0.8 (GeV/c)^2 and 0.8-1.1 (GeV/c)^2, and 1.4-2.1 GeV for the highest Q^2 bin, 1.1-1.5 (GeV/c)^2. Data were corrected for acceptance, reconstruction efficiency, radiative effects, and empty target counts [8]. In particular, a specifically developed Monte Carlo code was used to calculate the acceptance and efficiency. To this purpose, event distributions were generated in a realistic way and then processed through the GEANT-based code describing detector interactions. The same Monte Carlo event generator was used to perform extrapolations to kinematic regions where the acceptance vanishes. This type of corrections was typically only a few percent of the total cross section measured. Data were binned in the following set of hadronic CM variables: invariant mass of the $p\pi^+$ pair (10 bins), invariant mass of the $\pi^+\pi^-$ pair (10 bins), π^- polar angle θ (10 bins), azimuthal angle ϕ (5 bins), and rotation freedom ψ of the $p\pi^+$ pair with respect to the hadronic plane (5 bins). The full differential cross section is of the form:

$$\frac{d\sigma}{dW dQ^2 dM_{p\pi^+} dM_{\pi^+\pi^-} d\cos\theta_{\pi^-} d\phi_{\pi^-} d\psi_{p\pi^+}} =$$

$$\Gamma_v \frac{d\sigma_v}{dM_{p\pi^+} dM_{\pi^+\pi^-} d\cos\theta_{\pi^-} d\phi_{\pi^-} d\psi_{p\pi^+}} = \Gamma_v \frac{d\sigma_v}{d\tau} \quad (1)$$

$$\Gamma_v = \frac{\alpha}{4\pi} \frac{1}{E^2 M_p^2} \frac{W(W^2 - M_p^2)}{(1-\epsilon)Q^2} \quad (2)$$

where Γ_v is the virtual photon flux, $\frac{d\sigma_v}{d\tau}$ is the virtual photon cross section, α is the fine structure constant, E is the electron beam energy, M_p is the proton mass, and ϵ is the virtual photon transverse polarization [9]. Systematic

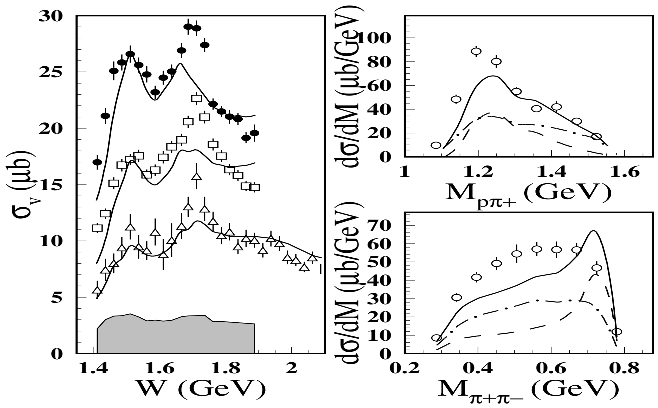

FIG. 1: Left: Total cross section for $\gamma_v p \to p\pi^+\pi^-$ as a function of W. Data from CLAS are shown at Q^2=0.5-0.8 (GeV/c)^2 (full points), Q^2=0.8-1.1 (GeV/c)^2 (open squares), and Q^2=1.1-1.5 (GeV/c)^2 (open triangles). Error bars are statistical only, while the bottom band shows the sytematic error for the lowest Q^2 bin. The curves represent our step (A) reference calculations. Right: $\frac{d\sigma_v}{dM_{p\pi^+}}$ (top) and $\frac{d\sigma_v}{dM_{\pi^+\pi^-}}$ (bottom) from CLAS at Q^2=0.8-1.1 (GeV/c)^2 and W=1.7-1.725 GeV (statistical error bars only). The curves represent our step (A) reference calculations, extrapolated to the edge points. The dashed line includes all resonances, the dot-dashed line includes only the non-resonant part, and the solid line is the full calculation.

uncertainties were estimated as a function of W and Q^2. The main sources were acceptance modeling, finite integration steps, and modeling of the radiative corrections, each one being at the 3 to 10% level. Each of the various cuts applied (fiducial, missing mass, etc.) contributed 2 to 5%. In Fig. 1 (left) we report the total virtual photon cross section as a function of W for all Q^2 intervals analyzed. The CLAS data points clearly exhibit structures, not visible in previous data [10] due to limited statistical accuracy.

Since existing theoretical models [11] are limited to W <1.6 GeV, we have employed a phenomenological calculation [12] for a first interpretation of the data. This model describes the reaction $\gamma_v p \to p\pi^+\pi^-$ in the kinematic range of interest as a sum of amplitudes for $\gamma_v p \to \Delta\pi \to p\pi^+\pi^-$ and $\gamma_v p \to \rho^0 p \to p\pi^+\pi^-$, according to the structures observed in the final state invariant mass distributions, while all other possible mechanisms are parameterized as phase space. A detailed treatment was developed for the non-resonant contributions to $\Delta\pi$, while for ρp production they were described through a diffractive ansatz. For the resonant part, a total of 12 states, classified as 4* [1], with sizeable $\Delta\pi$ and/or ρp decays, were included based on a Breit-Wigner ansatz. A few model parameters in non-resonant production were fitted to CLAS data at high W, where the non-resonant part creates a forward peaking in the angular distributions, and kept fixed in the subsequent analysis. The phase between resonant and non-resonant $\Delta\pi$ mechanisms was fitted to the CLAS data as well. To simplify the fits, we reduced eqn. (1) to three single-differential cross sections, the most sensitive to the dynamical content of our measurement [12], $\frac{d\sigma}{dM_{p\pi^+}}$, $\frac{d\sigma}{dM_{\pi^+\pi^-}}$, and $\frac{d\sigma}{d\cos\theta_{\pi^-}}$, by integrating over the other hadronic variables. These three 1-D distributions were then fitted simultaneously. For each W and Q^2 bin, a total of 26 data points from the three single-differential cross sections were used in our fits.

The physics analysis included the following steps: (A) We produced reference curves using the available information on the N^* and Δ resonances in 1.2-2 GeV mass range. Discrepancies between the CLAS data and our calculation were observed, which led to the subsequent steps B and C. (B) Data around W=1.7 GeV were fitted using the known resonances in the PDG but allowing the resonance parameters to vary in a number of ways. The best fit, corresponding to a prominent P_{13} partial wave, could be attributed to the PDG $P_{13}(1720)$ resonance, but with parameters significantly modified from the PDG values. (C) As an alternative description, we introduced a new baryon state around 1.7 GeV. In what follows we describe each of the steps above in more detail.

Step (A) - To produce our reference curves, the Q^2 evolution of the $A_{1/2}$ and $A_{3/2}$ electromagnetic couplings for the states was taken either from parameterizations of existing data [13], or from Single Quark Transition Model (SQTM) fits [13] where no data were available. For the $P_{11}(1440)$ (Roper), given the scarce available data, the amplitude $A_{1/2}$ was taken from a Non-Relativistic Quark Model (NRQM) [14]. Partial LS decay widths were taken from a previous analysis of hadronic data [15] and renormalized to the total widths from Ref. [1]. Results for step (A) are reported in Fig. 1. The total cross section strength for W < 1.65 GeV (except for the region close to threshold), and for W > 1.8 GeV is well reproduced. In reference [8], a broader comparison to the differential cross sections is reported, showing that we were able to reproduce the main features of the measurement for W < 1.65 GeV and for W > 1.8 GeV. Instead, a strong discrepancy is evident at W around 1.7 GeV. Moreover, at this energy the reference curve exhibits a lack of $\Delta\pi$ strength in the $p\pi^+$ invariant mass (Fig. 1, right top), and a strong peak in the $\pi^+\pi^-$ invariant mass (Fig. 1,

TABLE I: PDG $P_{13}(1720)$ parameters from fit (B) and new state parameters from fit (C). Errors are statistical.

	M (MeV)	Γ (MeV)	$\frac{\Gamma_{\pi\Delta}}{\Gamma}$ (%)	$\frac{\Gamma_{\rho N}}{\Gamma}$ (%)
PDG P_{13} (B)	1725±20	114±19	63±12	19±9
PDG [1]	1650-1750	100-200	N/A	70-85
new P_{13} (C)	1720±20	88±17	41±13	17±10

right bottom), connected to sizeable ρ meson production. The latter was traced back to the 70-91% branching ratio of the $P_{13}(1720)$ into this channel [1, 15, 16].

Step (B) - We then considered whether the observed discrepancy around 1.7 GeV could be accomodated by varying the electromagnetic excitation of one or more of the PDG states. In our code, interference effects between continuum and resonances like those reported in Ref. [11], are taken into account automatically inside the model frame [12]. Therefore, our investigation at this stage was including the possibility of accounting for the 1.7 GeV structure via interference effects, although the peaking of such an interference pattern at the same W for all Q^2 bins would be rather surprising. Assuming the resonance properties given by the PDG, the bump at about W=1.7 GeV cannot be due to the $D_{15}(1675)$, $F_{15}(1680)$, or $D_{33}(1700)$ states; the first because its well known position cannot match the peak; the second because of its well known position and photocouplings [17]; the third due to its large width (∼300 MeV). The remaining possibilities from the PDG are the $D_{13}(1700)$, the $P_{13}(1720)$, and the $P_{11}(1710)$ (the latter was not included in step (A)), as there are no data available on the Q^2 dependence of $A_{1/2}$ or $A_{3/2}$ [17]. If no configuration mixing occurs, the $D_{13}(1700)$ cannot be excited in the SQTM from proton targets, while the SQTM prediction for the $P_{13}(1720)$ relies on ad hoc assumptions. According to the literature [1, 15, 16], hadronic couplings of the $D_{13}(1700)$ and the total width of the $P_{11}(1710)$ are poorly known, while the $P_{13}(1720)$ hadronic parameters should be better established. Therefore our next step was to allow for a variation of the properties of these three states, in order to fit the data. Several other partial waves were investigated in step (C). Before proceeding with such fits, we performed slight variations of the initial curves from step (A), as allowed by the uncertainties in the knowledge of a number of states. All fit χ^2/ν values were calculated from the 8 W bins between 1.64 and 1.81 GeV and from the 3 Q^2 bins (624 data points). The number of free parameters ranged from 11 to 32, depending on the fit, corresponding to ν=613 to 592 degrees of freedom.

We first performed three separate fits, (B1), (B2), and (B3), where the photo- and hadronic couplings of only one resonance at a time were widely varied, specifically the $D_{13}(1700)$ for (B1), the $P_{13}(1720)$ for (B2), and the $P_{11}(1710)$ for (B3). Fits (B1) and (B3) gave a poor description of the data, with χ^2/ν=5.2 and 4.3, respectively. The best fit (χ^2/ν =3.4) was obtained in (B2)

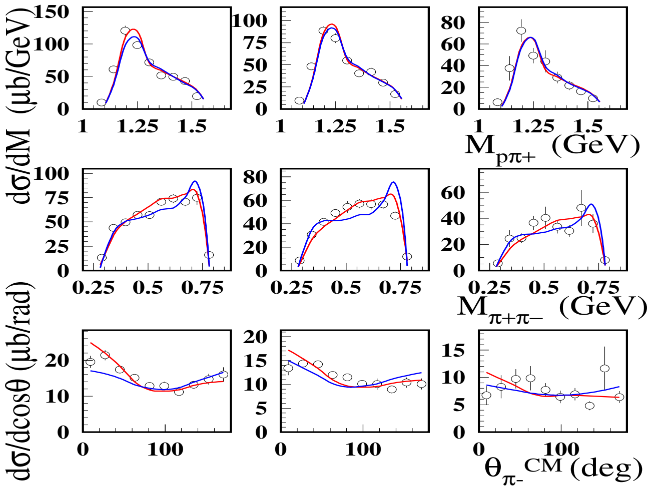

FIG. 2: $\frac{d\sigma_v}{dM_{p\pi^+}}$, $\frac{d\sigma_v}{dM_{\pi^+\pi^-}}$, and $\frac{d\sigma_v}{dcos\theta_{\pi^-}}$ from CLAS (from top to bottom) at W=1.7-1.725 GeV and for the three mentioned Q^2 intervals (left to right). The error bars include statistical errors only. Curves (see text) correspond to the fits (B2) (red), and (B4) (blue), and are extrapolated to the mass distributions edge points.

(Fig. 2). However, the resulting values for the branching fractions of the $P_{13}(1720)$ were significantly different from previous analyses reported in the literature and well outside the reported errors [1, 15, 16]. In a final multiresonance fit (B4), we varied the photocouplings of all three candidate states, keeping the hadronic couplings inside the published uncertainties. No better solution was found, the χ^2/ν being 4.3 (Fig. 2), worse than (B2). In Fig. 3 we report the final comparison of fits (B2) and (B4) with the total cross section data. Table I (first row)

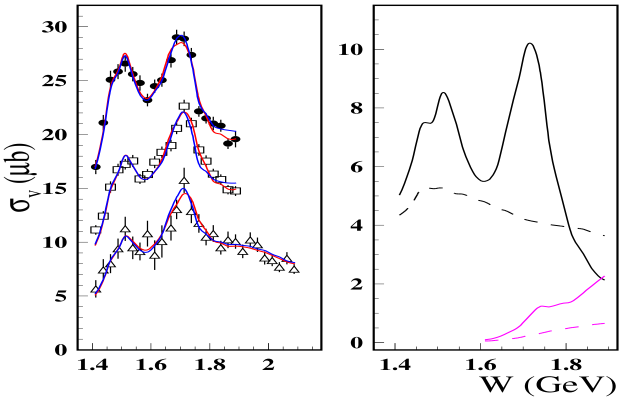

FIG. 3: Left: Total cross section for $\gamma_v p \to p\pi^+\pi^-$ as a function of W from CLAS at the 3 mentioned Q^2 intervals (see fig.1). The error bars are statistical only. The curves (see text) correspond to the fits (B2) (red), and (B4) (blue). Right: subdivision of the fitted cross section (B2) for Q^2=0.5-0.8 (GeV/c)^2 into resonant $\Delta^{++}\pi^-$ (black solid), continuum $\Delta^{++}\pi^-$ (black dashed), resonant $\rho^0 p$ (magenta solid), and continuum $\rho^0 p$ (magenta dashed). Notice the different vertical scales.

shows our (B2) results for the hadronic couplings of the $P_{13}(1720)$, in comparison with the PDG values (second

TABLE II: PDG $P_{13}(1720)$ total photocoupling from fit (B2) and new state total photocoupling from fit (C). Errors are statistical.

step	Q^2 $(\mathrm{GeV/c})^2$	$\sqrt{A^2_{1/2}+A^2_{3/2}+S^2_{1/2}}$ $(10^{-3}/\sqrt{\mathrm{GeV}})$
B2	0.65	83±5
B2	0.95	63±8
B2	1.30	45±27
C	0.65	76±9
C	0.95	54±7
C	1.30	41±18

row), while Table II shows our (B2) results for its total photocoupling strength (first three rows).

As discussed above, fitting the data around 1.7 GeV with established baryon states leads either to a poor fit or to a drastic change in resonance parameters with respect to published results. In the framework of our analysis, there is no way to assess the reliability of the previously determined hadronic parameters of the PDG $P_{13}(1720)$. The resonant content of the reaction $\pi N \to \pi\pi N$, which is used to obtain the hadronic parameters, may be different from that of reactions initiated by an electromagnetic probe. In particular, the $P_{13}(1720)$ state seen in $\pi N \to \pi\pi N$ may not be excited in electroproduction, while some other state that decouples from πN may be excited electromagnetically. This possibility is studied in the next step.

Step (C) - We investigated whether our data could be fitted by including another baryon state, while keeping the hadronic parameters of the $P_{13}(1720)$ as in Refs. [1, 15]. The quantum numbers S_{I1},P_{I1},P_{I3},D_{I3},D_{I5}, F_{I5},F_{I7} were tested on an equal footing, where $I/2$ is the isospin, undetermined in our measurement. The total decay width of the new state was varied in the range of 40-600 MeV, while its position was varied from 1.68 to 1.76 GeV. The best fit (χ^2/ν=3.3) was obtained with a P_{I3} state, while other partial waves gave a $\chi^2/\nu \geq 4.2$. Curves obtained from the best fit were nearly identical with the red solid lines in Figs. 2 and 3. In order to avoid the unobserved ρ production peak (Fig. 1, right), the PDG $P_{13}(1720)$ state had to be suppressed, making its contribution very small. Instead, in this fit the main contribution to the bump came from the new state. Resonance parameters and total photocoupling value obtained from the assumed new state are reported in Table I (last row) and II (last 3 rows), respectively.

A second P_{13} state was indeed predicted in Ref. [4], with a mass of 1870 MeV, and in Ref. [18], with a mass of 1816 MeV. The presence of a new three-quark state with the same quantum numbers as the conventional $P_{13}(1720)$ in the same mass range would likely lead to strong mixing. However, as mentioned above, a different isospin cannot be excluded. The new state may also have a different internal structure, such as a hybrid baryon with excited glue components. Such a P_{13} hybrid state is predicted in the flux tube model [19]. Finally, in Ref. [20] the existence of a P_{13} pentaquark ($qqqq\bar{q}$) configuration with a mass in the range 1.76-1.78 GeV is predicted. Yet another possibility is that some resonance parameters established in previous analyses may have much larger uncertainties than reported in the literature. In this case, outlined in our step (B), our analysis would establish new, more precise parameters for a known state, and invalidate previous results.

In conclusion, in this letter we presented data on the $ep \to e'p\pi^+\pi^-$ reaction in a wide kinematic range, with higher quality than any previous double pion production experiment. Our phenomenological calculations using existing PDG parameters provided a general good agreement with the new data, expect for the structure at $W \sim$ 1700 MeV. We explored two alternative interpretations of the data. If we dismiss previously established hadronic parameters for the $P_{13}(1720)$ we can fit the data with a state having the same spin/parity/isospin but strongly different hadronic couplings from the PDG state. If, alternatively, we introduce a new state in addition to the PDG state with about the same mass, spin $\frac{3}{2}$, and positive parity, a good fit is obtained for a state having a rather narrow width, a strong $\Delta\pi$ coupling, and a small ρN coupling, while keeping the PDG $P_{13}(1720)$ hadronic parameters at published values. In either case we determined the total photocoupling at $Q^2 > 0$. A simultaneous analysis of single and double-pion processes provides more constraints and may help discriminate better between alternative interpretations of the observed resonance structure in the CLAS data. Such an effort is currently underway.

We would like to acknowledge the outstanding efforts of the staff of the Accelerator and the Physics Divisions at JLab that made this experiment possible. This work was supported in part by the Istituto Nazionale di Fisica Nucleare, the U.S. Department of Energy and National Science Foundation, the French Commissariat à l'Energie Atomique, and the Korea Science and Engineering Foundation. U. Thoma acknowledges an "Emmy Noether" grant from the Deutsche Forschungsgemeinschaft. The Southeastern Universities Research Association (SURA) operates the Thomas Jefferson National Accelerator Facility for the United States Department of Energy under contract DE-AC05-84ER40150.

[1] D.E. Groom *et al.*, Eur. Phys. J. **C15**, 1 (2000).
[2] R. Koniuk and N. Isgur, Phys. Rev. Lett. **44**, 845 (1980); Phys. Rev. **D21**, 1868 (1980).
[3] M.M. Giannini, Rep. Prog. Phys. **54**, 453 (1991).

[4] S. Capstick, W. Roberts, Phys. Rev. **D49**, 4570 (1994).
[5] F. Stancu and P Stassart, Phys. Rev. **D47**, 2140 (1993).
[6] M. Kirchbach, Mod.Phys.Lett. **A12**, 3177 (1997).
[7] B. Mecking et al., accepted for publication in: Nucl. Inst. and Meth. A; W. Brooks, Proc. of PANIC '99, Uppsala, Sweden, 10-16 June 1999, Nucl. Phys. **A 663&664**, 29c (2000).
[8] M. Ripani et al., hep-ex/0304034.
[9] E. Amaldi, S. Fubini, and G. Furlan, Pion Electroproduction, Springer Tracts in Modern Physics **83** (1989).
[10] V. Eckart *et al.*, Nucl. Phys. **B55**, 45 (1973); P. Joos *et al.*, Phys. Lett. **B52**, 481 (1974); K. Wacker *et al.*, Nucl. Phys. **B144**, 269 (1978).
[11] J.C. Nacher and E. Oset, Nucl. Phys. **A674**, 205 (2000), and related work referenced therein.
[12] M. Ripani *et al.*, Nucl. Phys. **A672**, 220 (2000); V. Mokeev *et al.*, Phys. of Atomic Nucl. **64**, 1292 (2001); V. Mokeev *et al.*, to be published in Phys. of Atomic Nucl.
[13] V.D. Burkert, Czech. Journ. of Phys. **46**, 627 (1996).
[14] F. Close and Z.P. Li, Phys. Rev. **D42**, 2194 (1990).
[15] D.M. Manley, E.M. Saleski, Phys. Rev. **D45**, 4002 (1992).
[16] T.P. Vrana *et al.*, Phys. Rept. **328**, 181 (2000).
[17] V. Burkert, Nucl. Phys. **A684**, 16c (2001).
[18] M.M. Giannini et al., Eur. Phys. J. **A12**, 447 (2001).
[19] S. Capstick, P. Page, Phys. Rev. **C66**, 065204 (2002).
[20] H. Walliser, V.B. Kopeliovich., hep-ph/0304058.